Protein Science (2000), *9*:2151–2160. Cambridge University Press. Printed in the USA.

Position effect of cross-strand side-chain interactions on β-hairpin formation

CLARA M. SANTIVERI, MANUEL RICO, AND M. ANGELES JIMÉNEZ

Instituto de Estructura de la Materia, Consejo Superior de Investigaciones Científicas, Serrano 119, 28006-Madrid, Spain

(RECEIVED January 3, 2000; FINAL REVISION September 1, 2000; ACCEPTED September 1, 2000)

Abstract

Previous conformational analysis of 10-residue linear peptides enabled us to identify some cross-strand side-chain interactions that stabilize β-hairpin conformations. The stabilizing influence of these interactions appeared to be greatly reduced when the interaction was located at the N- and C-termini of these 10-residue peptides. To investigate the effect of the position relative to the turn of favorable interactions on β-hairpin formation, we have designed two 15-residue β-hairpin forming peptides with the same residue composition and differing only in the location of two residues within the strand region. The conformational properties of these two peptides in aqueous solution were studied by ^{1}H and ^{13}C NMR. Differences in the conformational behavior of the two designed 15-residue peptides suggest that the influence of stabilizing factors for β-hairpin formation, in particular, cross-strand side-chain interactions, depends on their proximity to the turn. Residues adjacent to the turn are most efficient in that concern. This result agrees with the proposal that the turn region acts as the driving force in β-hairpin folding.

Keywords: β-hairpin; β-turn; NMR; peptide design; protein folding; side-chain interactions

Understanding the forces that govern the formation and stability of secondary structure is essential for the rational and successful de novo design of proteins. Analysis of the conformational behavior of protein fragments and designed peptides has provided a large amount of information on the formation and stability of α-helices (Scholtz & Baldwin, 1992; Lyu et al., 1993; Zhou et al., 1993; Baldwin, 1995; Muñoz & Serrano, 1997; Aurora & Rose, 1998). However, experimental data on peptides adopting monomeric β-sheet motifs in aqueous solution have been reported only in the 1990s (see reviews by Smith & Regan, 1997; Blanco et al., 1998; Gellman, 1998; Lacroix et al., 1999; and references therein), probably because sequences with high β-sheet propensities tend to aggregate. Since the publication of the first designed β-hairpin-forming peptide (Blanco et al., 1993), the design of short linear peptides able to form β-sheets has become a subject of intense activity. Most of the β-sheet-forming peptides reported to date adopt a β-hairpin motif, the simplest antiparallel β-sheet structure consisting of two antiparallel hydrogen-bonded β-strands linked by a turn region. β-Hairpin motifs differ in the length of the turn region and are classified according to the number of turn residues and the hydrogen bond pattern of residues flanking the turn (Sibanda & Thornton, 1985, 1991; Sibanda et al., 1989). Several studies on model peptides highlighted the importance of the turn region in determining β-hairpin stability (Ramírez-Alvarado et al., 1997; Blanco et al., 1998; Gellman, 1998; Griffiths-Jones et al., 1999). Moreover, the NMR investigation of a series of model β-hairpin-forming peptides (de Alba et al., 1996, 1997a, 1999a), showing that they were able to adopt different β-hairpin structures when differing only on their turn sequence, demonstrated that the turn sequence determines the β-strand alignment in the β-hairpin. Further evidence came from ubiquitin-derived peptides that showed different strand register depending on the turn residues (Searle et al., 1995; Haque & Gellman, 1997). Cross-strand side-chain interactions are, at least in our studied peptide system, less relevant for β-hairpin formation (de Alba et al., 1997b), though they certainly contribute to β-hairpin stability (Ramírez-Alvarado et al., 1996, 1999; Blanco et al., 1998; Gellman, 1998). We have indeed identified some favorable and unfavorable cross-strand side-chain interactions from the conformational analysis of a series of decapeptides able to form β-hairpins (de Alba et al., 1997b). In that study, the influence of cross-strand side-chain interactions on β-hairpin stability appeared to vanish when the interaction was placed at the N- and C-termini. To investigate how the location of cross-strand side-chain interactions relative to the turn region af-

Reprint requests to: M. Angeles Jiménez, Instituto de Estructura de la Materia, Consejo Superior de Investigaciones Científicas, Serrano 119, 28006-Madrid, Spain; e-mail: angeles@malika.iem.csic.es

Abbreviations: 1D, one-dimensional; 2D, two-dimensional; $\Delta\delta$ ($= \delta_{observed} - \delta_{random\ coil}$), conformational shift; COSY, homonuclear correlated spectroscopy; HSQC, heteronuclear single quantum coherence spectroscopy; M_{av}, average molecular weight; M_{th}, theoretical molecular weight; NOE, nuclear Overhauser enhancement; NOESY, nuclear Overhauser enhancement spectroscopy; ppm, parts per million; RMSD, root-mean-square deviation; ROESY, rotating frame NOE spectroscopy; TOCSY, total correlation spectroscopy; TSP, sodium [3-trimethylsilyl 2,2,3,3-^{2}H] propionate.

Peptide 1		**I**	Y	**S**	N	S	D	G	T	W	T		
Peptide 2		**S**	Y	**I**	N	S	D	G	T	W	T		
Peptide 3	S E	**I**	Y	**S**	N	S	D	G	T	W	T	V T E	
Peptide 4	S E	**S**	Y	**I**	N	S	D	G	T	W	T	V T E	

Fig. 1. Peptide sequences. Residues that lengthen peptides 3–4 relative to peptides 1–2 are underlined and those located at different positions in peptides 1 and 3 relative to peptides 2 and 4, respectively, are in bold.

fects their effect on β-hairpin formation, we have designed two longer β-hairpin forming peptides. These peptides have the same amino acid composition and differ only in the position of two residues at the N-terminal strand. In this paper, we describe the design and NMR conformational investigation of these two 15-residue peptides. Analysis of the conformational properties of these pentadecapeptides indicates that the contribution of cross-strand side-chain interactions to β-hairpin formation depends on their relative position to the turn, being more stabilizing, if favorable, and more destabilizing, if unfavorable, when closer to the turn.

Results

Peptide design

Pentadecapeptides 3 and 4 were designed by adding two and three residues at the N- and C-termini, respectively, of the β-hairpin forming decapeptides 1 and 2 (de Alba et al., 1997b; Fig. 1). The β-hairpin conformations adopted by these peptides are schematically shown in Figure 2. β-Sheet propensities and solubility criteria were considered in selecting the five new residues, the sequences SE and VTE added to the N- and C-end, respectively. They contain two residues (V and T) with high intrinsic β-sheet propensities (Chou & Fasman, 1974; Kim & Berg, 1993; Minor & Kim, 1994; Muñoz & Serrano, 1994; Smith et al., 1994; Swindells et al., 1995), an S residue that is the most hydrophilic residue with some β-sheet propensity, and two E residues whose charges should improve peptide solubility.

Aggregation test

The absence of aggregation in peptides 3 and 4 in aqueous solution was checked by recording 1D ^{1}H NMR spectra of peptides 3 and 4 at two different concentrations, 2 and 0.2 mM. The linewidths

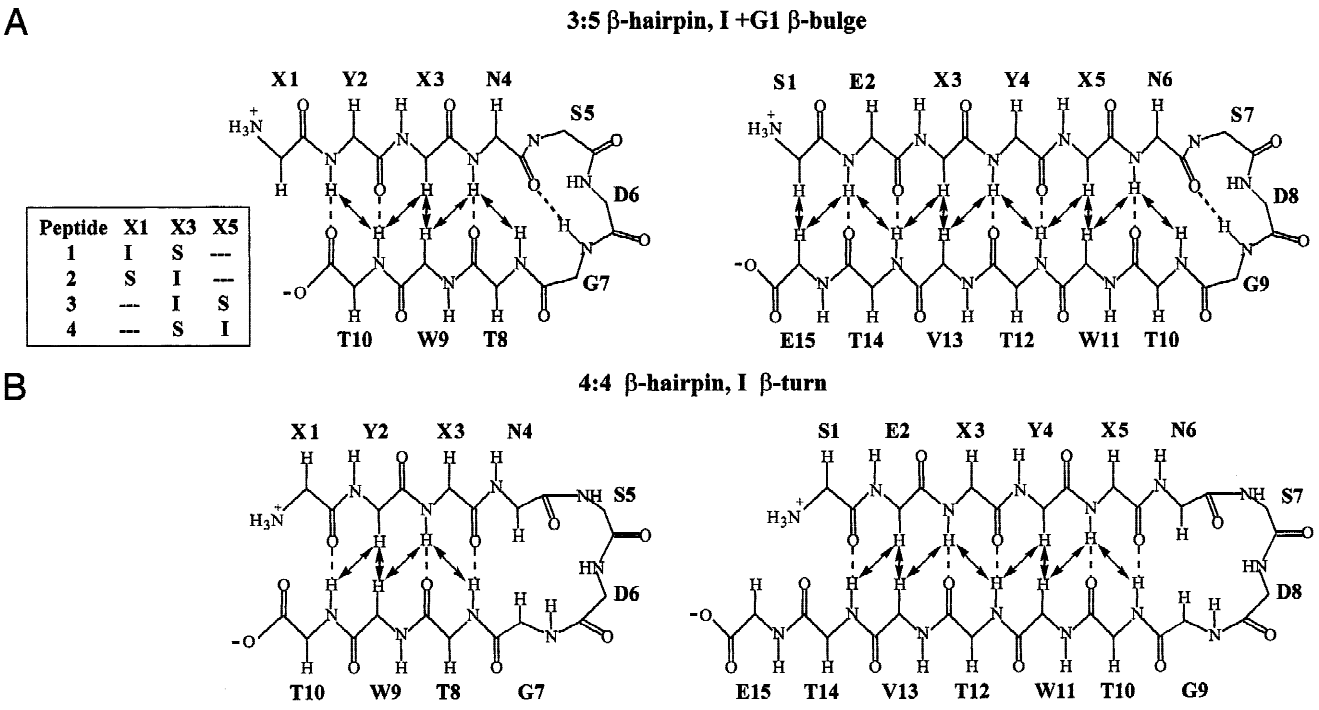

Fig. 2. Schematic representation of the peptide backbone conformations of (**A**) the 3:5 β-hairpin formed by peptides 1–2 (left) and expected for peptides 3–4 (right), and (**B**) the 4:4 β-hairpin formed by peptide 1 (left) and expected for peptides 3–4 (right). β-Sheet hydrogen bonds are indicated by dotted lines and the expected long-range NOEs involving backbone protons by black arrows. A pair of facing residues is in a hydrogen bonded site when their CO and NH are hydrogen bonded, and in a nonhydrogen bonded site when they are not hydrogen bonded.

and chemical shifts at the two concentrations were identical, indicating the monomeric state of the two peptides. The similarity between the average molecular weights obtained from sedimentation equilibrium experiments performed with the dilute samples of the peptides and the molecular weights calculated on the basis of the amino acid composition provided further confirmation of their monomeric state (peptide 3, $M_{th}/M_{av} = 1.09$; peptide 4, $M_{th}/M_{av} = 0.97$).

C_αH conformational shifts

The C_αH conformational shift profiles ($\Delta\delta_{C\alpha H} = \delta_{observed} - \delta_{random\ coil}$) of peptides 3 and 4 (Fig. 3) present negative values at residues 7–9 that are indicative of a chain-bend region, and positive values at residues 2–6 and 10–14 as expected for β-strands region (Case et al., 1994; Wishart & Sykes, 1994; Szilágyi, 1995). The N- and C-terminal residues are excluded due to charged end effects. Therefore, with the single exception of the residue at position 5, the $\Delta\delta_{C\alpha H}$ profiles observed for peptides 3 and 4 are characteristic of β-hairpins.

The $\Delta\delta_{C\alpha H}$ profiles expected for a 4:4 β-hairpin and for a 3:5 β-hairpin, the type of hairpins that peptides 3 and 4 will most probably adopt, differ at a single position. The ϕ and ψ angles of the first turn residue, N6 in peptides 3 and 4, are in the β-region of the Ramachandran map in a 3:5 β-hairpin and in the α_R region in a 4:4 β-hairpin (Sibanda & Thornton, 1991) that leads, respectively, to positive and negative $\Delta\delta_{C\alpha H}$ values. The positive $\Delta\delta_{C\alpha H}$ value that is observed for the N6 residue in peptide 4 (Fig. 3) indicates the presence of a 3:5 β-hairpin. The almost zero $\Delta\delta_{C\alpha H}$ value observed for residue N6 of peptide 3 (Fig. 3), however, suggests that peptide 3 is adopting a 3:5 and a 4:4 β-hairpin, since a population-weighted average $\Delta\delta_{C\alpha H}$ value is expected in the presence of the two β-hairpins. The evidence about the type of β-hairpin provided by the $\Delta\delta_{C\alpha H}$ profiles, in particular when a mixture of different β-hairpins can coexist, is not unambiguous, but it is useful to check their consistency with other NMR parameters.

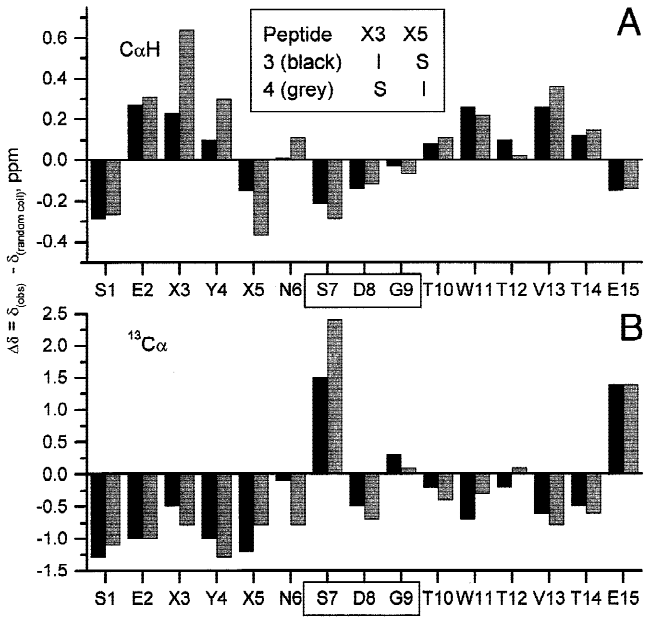

Fig. 3. (**A**) C_αH and (**B**) $^{13}C_\alpha$ conformational shifts ($\Delta\delta = \delta_{(obs)} - \delta_{(random\ coil)}$, ppm, where $\delta_{C\alpha H(random\ coil)}$ were taken from Bundi and Wüthrich (1979) and $\delta_{^{13}C_\alpha(random\ coil)}$ from Wishart et al., 1995) as a function of sequence for peptides 3 (in black) and 4 (in grey) at pH 5.5 and 5 °C. For Gly, the $\Delta\delta_{C\alpha H}$ shown corresponds to the average value of the two α-protons. Turn residues in the 3:5 β-hairpin formed by peptides 3 and 4 are boxed. Inset shows the X3 and X5 amino acids corresponding to peptides 3 and 4. The $\Delta\delta_{C\alpha H}$ and $\Delta\delta^{13}{}_{C_\alpha}$ values shown for W11 in peptide 3 are at pH 5.5 and 20 °C because C_αH signal is under water resonance at 5 °C.

$^{13}C_\alpha$ conformational shifts

The $^{13}C_\alpha$ conformational shifts ($\Delta\delta^{13}{}_{C\alpha} = \delta_{observed} - \delta_{random\ coil}$) have been recognized as a useful and sensitive parameter to detect and identify secondary structure (Buckley et al., 1993; Gronenborn & Clore, 1994; Yao et al., 1997; Guerois et al., 1998). Since the main factors affecting the $^{13}C_\alpha$ chemical shifts are the ϕ and ψ backbone dihedral angles (Spera & Bax, 1991; de Dios et al., 1993; Wishart & Sykes, 1994; Szilágyi, 1995; Iwadate et al., 1999), they are less dependent on ring current effects than the C_αH chemical shifts.

The $\Delta\delta^{13}{}_{C_\alpha}$ profiles of peptides 3 and 4 (Fig. 3) are negative at residues 2–6 and 10–14 as expected for β-strands (Spera & Bax, 1991; de Dios et al., 1993; Wishart & Sykes, 1994; Szilágyi, 1995; Iwadate et al., 1999). As in the case of $\Delta\delta_{C\alpha H}$ profiles, we do not consider the N- and C-terminal residues. With regard to the turn region, there is a large positive value for S7, the $i + 1$ turn residue, a negative value for D8, the $i + 2$ residue, and a slightly positive value for G9, the $i + 3$ turn residue. This is the $\Delta\delta^{13}{}_{C_\alpha}$ pattern expected for 3:5 and 4:4 β-hairpins considering their characteristic ϕ and ψ angles (Sibanda & Thornton, 1991) and the effect of backbone dihedral angles on the $\delta^{13}{}_{C_\alpha}$ value (Spera & Bax, 1991; Iwadate et al., 1999). According to it, the $\Delta\delta^{13}{}_{C_\alpha}$ values at the first turn residue, N6 in peptides 3 and 4, are expected to be negative in 3:5 β-hairpins and positive in 4:4 β-hairpins. Therefore, the negative $\Delta\delta^{13}{}_{C_\alpha}$ and large (in absolute value) found for the N6 residue in peptide 4 (Fig. 3) indicates the presence of a 3:5 β-hairpin. The almost null $\Delta\delta^{13}{}_{C_\alpha}$ value observed for N6 in peptide 3 is consistent with a mixture of 3:5 and 4:4 β-hairpins, because a population-weighted average $\Delta\delta^{13}{}_{C_\alpha}$ value is expected in the presence of the two β-hairpins, as in the case of $\Delta\delta_{C\alpha H}$ conformational shifts.

NOE data

NOE data provide the most conclusive NMR evidence for the formation of β-hairpin structures. The set of observed NOEs per-

Table 1. *Peptide sequences and populations of β-hairpin conformations formed by peptides 1-4 in D_2O*[a]

Peptide	4:4 β-hairpin strand						Turn		Population estimated from NOE intensity[b]	3:5 β-hairpin strand						Turn		Population estimated from NOE intensity[b]
1[c]				I1	Y2	S3	**N4**	**S5**				I1	Y2	S3	N4	**S5**		
				‖		‖			32%				‖		|		**D6**	27%
				T10	W9	T8	**G7**	**D6**					T10	W9	T8	**G7**		
2[c]				S1	Y2	I3	**N4**	**S5**				S1	Y2	I3	N4	**S5**		
				‖		‖			Nondetected				‖		|		**D6**	47%
				T10	W9	T8	**G7**	**D6**					T10	W9	T8	**G7**		
3[d]		S1	E2	I3	Y4	S5	**N6**	**S7**		S1	E2	I3	Y4	S5	N6	**S7**		
		‖		‖		‖			6%[e]		‖		‖		|		**D8**	13%[f]
	E15	T14	V13	T12	W11	T10	**G9**	**D8**		E15	T14	V13	T12	W11	T10	**G9**		
4[g]		S1	E2	S3	Y4	I5	**N6**	**S7**		S1	E2	S3	Y4	I5	N6	**S7**		
		‖		‖		‖			Nondetected		‖		‖		|		**D8**	63%[h]
	E15	T14	V13	T12	W11	T10	**G9**	**D8**		E15	T14	V13	T12	W11	T10	**G9**		

[a]Turn residues are indicated in bold. Vertical lines indicate hydrogen bonds between strand residues. The differential cross-strand interactions between the hairpins adopted by peptides 3 and 4 are underlined. Data for peptides 1 and 2 were taken from de Alba et al. (1996, 1997b).
[b]As described in text.
[c]pH 6.3 and 2 °C.
[d]pH 4.3 and 20 °C.
[e]From C_αHE2-C_αHV13 NOE intensity.
[f]From C_αHS5-C_αHW11 NOE intensity.
[g]pH 5.5 and 5 °C.
[h]From the average of the populations obtained from the intensities of C_αHS3-C_αHV13 and C_αHI5-C_αHW11 NOEs.

mits the unambiguous determination of the strand register and the type of β-hairpin adopted by a given peptide, since different types of β-hairpin structures lead to different NOEs involving the backbone protons ($d_{\alpha\alpha(i,j)}$, $d_{\alpha N(i,j)}$, and $d_{NN(i,j)}$; Fig. 2). The NOE data described herein come from joint analysis of NOESY and ROESY spectra recorded under the same experimental conditions. ROESY experiments permit one to check whether a particular cross peak corresponds to a true NOE connectivity or to spin diffusion processes. The same set of NOE cross peaks was observed in the ROESY and NOESY spectra of peptides 3 and 4 under the same experimental conditions.

The NOESY spectrum of peptide 4 in aqueous solution shows long-range NOEs involving C_αH (C_αHS3-C_αHV13 and C_αHI5-C_αHW11; Fig. 4B) and amide protons (NHY4-NHT12) that are compatible with the formation of a single β-hairpin structure, the 3:5 β-hairpin (Fig. 2). The NOEs involving side-chain protons include NOEs between residues S3-V13, Y4-T12, and I5-W11 that face each other in the β-hairpin 3:5 and between S3-W11, Y4-N6, Y4-T14, W11-V13, and V13-E15 whose side chains are on the same side of the β-sheet (Table SM4 in Supplementary material in the Electronic Appendix). This provides further support for the formation of a 3:5 β-hairpin. No NOE indicative of even a small population of a 4:4 β-hairpin was detected.

In contrast, the pattern of NOEs observed for peptide 3 in aqueous solution is not compatible with a single preferred structure. The observed set of NOEs includes NHE2-NHT14 and C_αHS5-C_αHW11 NOEs indicative of a 3:5 β-hairpin, as well as a C_αHE2-C_αHV13 NOE characteristic of a 4:4 β-hairpin (Figs. 2, 4A; Table SM3 in Supplementary material in the Electronic Appendix). In addition, this peptide shows NOEs involving side-chain protons that can arise from a 3:5 β-hairpin, but are incompatible with a 4:4 β-hairpin, as well as NOEs compatible with a 4:4 β-hairpin, but not with a 3:5 β-hairpin (Table SM3 in Supplementary material in the Electronic Appendix).

Estimation of β-hairpin populations

Peptide 3 in aqueous solution at pH 4.3 and 20 °C adopts about 6% of a 4:4 β-hairpin and 13% of a 3:5 β-hairpin, as estimated from the C_αHE2-C_αHV13 and the C_αHS5-C_αHW11 NOE intensities (Table 1; see Materials and methods), respectively. These conformations coexist in equilibrium with the random coil. The other C_αH*i*-C_αH*j* NOEs characteristic of 4:4 and 3:5 β-hairpins (Fig. 2) could not be observed in peptide 3 due to signal overlapping. In aqueous solution at pH 5.5 and 5 °C, the fraction of peptide 4 forming a 3:5 β-hairpin is 63% (Table 1) on the basis of the C_αHI5-C_αHW11 and C_αHS3-C_αHV13 NOE intensities. The population estimated from the intensity of the C_αHI5-C_αHW11 NOE corresponding to the inner residues (73%) is slightly higher than that evaluated from the intensity of the C_αHS3-C_αHV13 NOE involving the residues at the middle of the strands (54%). This difference, though small, suggests the existence of an increasing flexibility at the strands when approaching the chain ends. This effect is analogous to the fraying observed in α-helical conformations (Baldwin, 1995), and it was previously observed in one β-hairpin forming peptide (de Alba et al., 1997a). Unfortunately, we could not measure the hairpin populations adopted by peptides 3 and 4 at identical conditions of pH and temperature due to overlap of the C_αH of W11 and the water signal (see below).

We have also evaluated the overall β-hairpin populations for the two peptides from the C_αH and the $^{13}C_\alpha$ conformational shifts observed in aqueous solution at pH 5.5 and 5 °C (Fig. 3), as described in Materials and methods. The evaluated values for peptide 4 are 62 and 51% of β-hairpin, as estimated from the C_αH and the

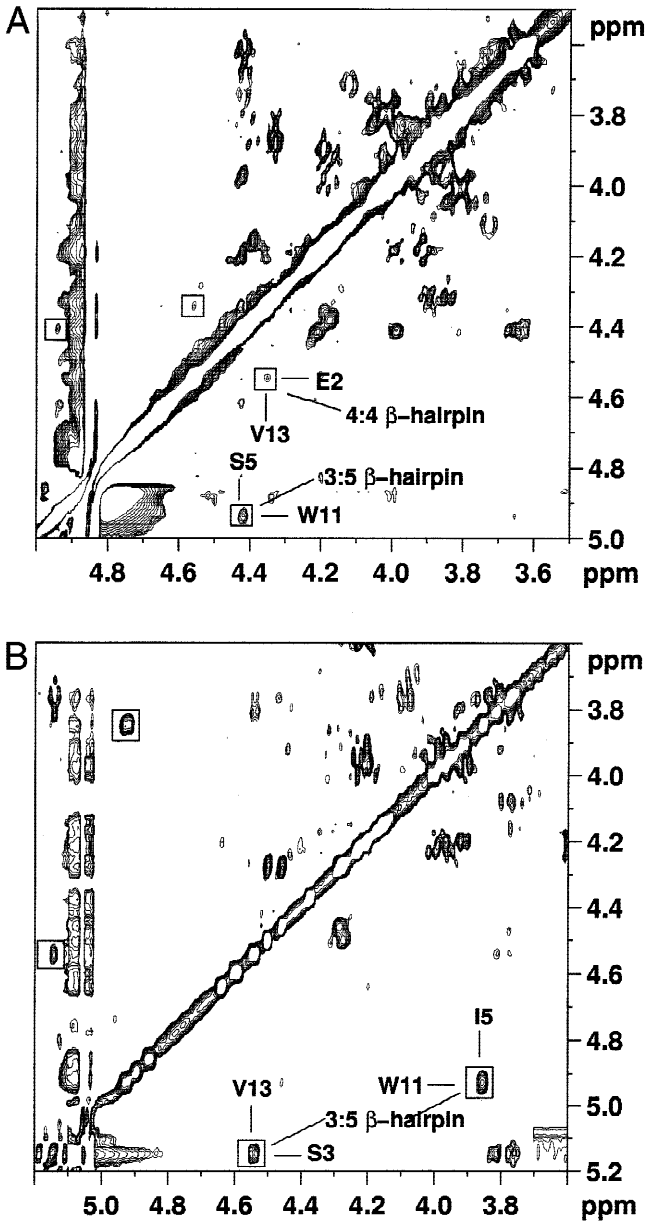

Fig. 4. Regions of NOESY spectra of (**A**) peptide 3 (2 mM, D_2O, pH 4.3, 20 °C, 200 ms mixing time) and (**B**) peptide 4 (2 mM, D_2O, pH 5.5, 5 °C, 200 ms mixing time). Nonsequential $C_\alpha H$-$C_\alpha H$ NOE cross peaks are boxed.

$^{13}C_\alpha$ conformational shifts, respectively, which is in good agreement with the population of 3:5 β-hairpin obtained from the NOE intensities (Table 1). The corresponding values for peptide 3 at pH 5.5 and 5 °C are 44 and 44%, as evaluated from the $C_\alpha H$ and the $^{13}C_\alpha$ conformational shifts, respectively. Taking into account that peptide 3 adopts a mixture of two β-hairpins (see above), these values correspond to the sum of the populations of 4:4 and 3:5 β-hairpins and are higher than the sum of the populations estimated from NOE intensities in spectra taken at 20 °C and pH 4.3 (Table 1). This result was expected since β-hairpin populations on one side increase at low temperature, and on the other the formation of β-hairpin is pH-dependent in peptides containing the NXDG sequence, where X is P or S, at the turn region, being the population of β-hairpin higher at pH 5.3 than at pH 4.3 (de Alba et al., 1995, 1996).

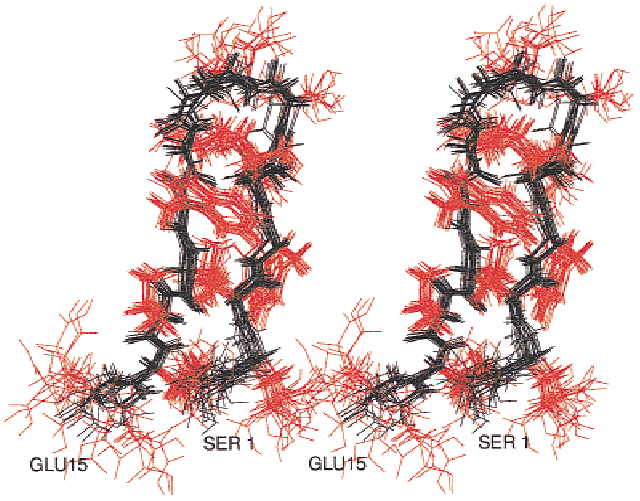

Fig. 5. Stereoscopic view of the superposition of all heavy atoms of the best 20 structures calculated for the 3:5 β-hairpin formed by peptide 4. Backbone atoms are shown in black and side-chain atoms in red.

Structure calculation

The high population of β-hairpin adopted by peptide 4 makes meaningful to perform a structure calculation. To this end, we used the distance restraints provided by the observed nonsequential NOEs (Table SM4 in Supplementary material in the Electronic Appendix), and the dihedral constraints coming from the large $^3J_{C\alpha H\text{-}NH}$ coupling constant measured for residues E2, Y4, T10, W11, T12, and V13 (>8 Hz) at the β-strands and the small $^3J_{C\alpha H\text{-}NH}$ found for residue S7 (<5 Hz) at the turn. Intraresidue and sequential NOEs were excluded because random coil conformations contribute to their intensities. The resulting structure is well defined. The RMSD of the best 20 calculated structures is 0.9 ± 0.2 Å for backbone atoms and 1.8 ± 0.4 Å for all heavy atoms (Fig. 5).

No structure calculation was performed for peptide 3 because of the co-existence of two β-hairpins in aqueous solution.

Discussion

The NMR conformational analysis of the peptides 3 and 4, whose sequences differ only in the position of two strand amino acids (Fig. 1), demonstrates their different abilities to form 3:5 and 4:4 β-hairpins (Table 1). Before going into the analysis of the factors contributing to the distinct conformational behavior of these two peptides, it is convenient to analyze the accuracy of the population estimates and the applicability of the two-state model to our peptide system.

Estimation of β-hairpin populations and validity of the two-state transition approximation

There is no well-established method to quantify the population of β-hairpin adopted by peptides (de Alba et al., 1996, 1997a, 1997b, 1999b; Ramírez-Alvarado et al., 1997, 1999; Blanco et al.,

1998; Gellman, 1998; Lacroix et al., 1999). The most widely used procedure is based on the intensity of the $C_\alpha H_i$-$C_\alpha H_j$ NOEs, where *i* and *j* are facing residues in a nonhydrogen-bonded site (Searle et al., 1995; de Alba et al., 1996, 1997a, 1997b; Ramírez-Alvarado et al., 1996; Maynard et al., 1998). Apart from the experimental error in the NOE intensity measurement, the main problem of this method lies in the fact that small differences in the actual $C_\alpha H_i$-$C_\alpha H_j$ distance relative to the reference value for the folded state (taken as the averaged value in antiparallel β-sheets in proteins) translate into large variations in population because NOE intensities are inversely proportional to the sixth power of the interproton distance. This dependence, however, makes correct the assumption that the $C_\alpha H_i$-$C_\alpha H_j$ distance in the unfolded state is large enough to make negligible the NOE intensity. Other error source is the potential existence of different local correlation times along the peptide chain and/or between the folded and the unfolded states. The overall β-hairpin populations can be independently evaluated on the basis of the $C_\alpha H$ and the $^{13}C_\alpha$ conformational shifts averaged over the β-strand residues since these shifts are dependent on the distinct environment corresponding to the different elements of secondary structure. The problems with the δ-based quantification methods arise from the lack of good reference values for both the random coil and the folded state (Ramírez-Alvarado et al., 1997, 1999; Gellman, 1998). Model peptides that are specific of the corresponding β-hairpin system (Ramírez-Alvarado et al., 1997; Syud et al., 1999) have been used as references. In analogy to the quantification of α-helical conformations (Jiménez et al., 1993, 1994; Muñoz et al., 1995; Lee & Cao, 1996), we have used as reference for the folded state the averaged $C_\alpha H$ conformational shifts observed in protein β-sheets (Wishart et al., 1991), and the δ-values measured in random coil tetrapeptides (Wüthrich, 1986) for the unfolded state. The use of the δ-values reported for other two different sets of nonstructured peptides (Merutka et al., 1995; Wishart et al., 1995) as reference for the unfolded state hardly varies the β-hairpin population estimates. Thus, the range obtained for the β-hairpin population evaluated for peptide 3 at pH 5.5 and 5 °C using the different random coil references is 44–50% and for peptide 4 under identical conditions 62–65%. $^{13}C_\alpha$ conformational shifts have been previously used to quantify β-sheet populations (de Alba et al., 1999b), taking as random coil values those reported by Wishart et al. (1995) and as reference for 100% β-hairpin the averaged $^{13}C_\alpha$ conformational shift observed in protein β-sheets (Spera & Bax, 1991). In the case of peptides that adopt a mixture of β-hairpins, as peptide 3, the populations estimated on the basis of δ values correspond to the total hairpin population, since the δ-values are linear averages over all the conformers in fast exchange. However, the characteristic NOEs of each type of hairpin are unique probes to separately quantify the corresponding population.

The δ-values of $^{13}C_\alpha$ carbons report on the local backbone conformation through their dependence on ϕ and ψ angles (Spera & Bax, 1991; de Dios et al., 1993; Case et al., 1994; Wishart & Sykes, 1994; Szilágyi, 1995; Iwadate et al., 1999), and any preferentially populated conformer will contribute to the observed δ-values. In contrast, the long-range NOEs, such as the $C_\alpha H_i$-$C_\alpha H_j$ NOE, arise only from those conformations, like the β-hairpins, with a short distance between the two protons. The agreement in the overall β-hairpin population evaluated for peptide 4 from $^{13}C_\alpha$ δ-values (probes for extended strands) with the one calculated from long-range $C_\alpha H_i$-$C_\alpha H_j$ NOEs (probes for proximity between the appropriate protons in the strands) strongly suggests a two-state behavior. Partially folded structures with, for example, one strand formed but no hairpin would lead to large $\Delta\delta_{^{13}C_\alpha}$ conformational shifts in absolute value and zero NOE intensity. Further evidence about two-state behavior would be provided by the practical coincidence of the individual residue estimates for the folded populations obtained by any quantification method. However, the lack of appropriate reference values for the folded and unfolded states (see above) is more problematic when considering individual residues. To circumvent this problem, the ratio between the $C_\alpha H$ conformational shifts at two different experimental conditions, what gives the ratio of populations at the two conditions, may be used (Maynard et al., 1998; Griffiths-Jones et al., 1999; Syud et al., 1999). β-Hairpin folding can be considered two-state if the obtained ratio is the same for all residues and equal to the ratio of the populations obtained by other quantification method. In that way, the reference for the folded state is not needed and only the errors in the reference for the unfolded state still affect the estimates of population. In peptide 4 in aqueous solution at pH 5.5, the overall β-hairpin population evaluated from the $C_\alpha H$ conformational shifts at the strands at 5 °C (62%, see above) is 1.9 times that at 35 °C (33%; see Materials and methods), and the ratio $\Delta\delta_{C\alpha H(5°C)}/\Delta\delta_{C\alpha H(35°C)}$ for each residue is within the range 1.5–2.7 (average ratio 2.1 ± 0.6). The exceptions are residues S1, D8, W11, T12, and E15, with a ratio close to 1, what is due to their $C_\alpha H$ δ-values being almost invariant with temperature, and T10, with a ratio of 3.7, which is affected by a large error due to its almost zero value for $\Delta\delta_{C\alpha H(35°C)}$, as found in other β-hairpin systems (Maynard et al., 1998; Griffiths-Jones et al., 1999). This result reinforces the idea that β-hairpin folding in peptide 4 approximates to a two-state transition.

Contributions to 4:4 and 3:5 β-hairpin formation in peptides 3 and 4

To investigate the effect of the position of stabilizing interactions relative to the turn in β-hairpin formation, we carried out the NMR conformational analysis of two peptides, 3 and 4, whose sequences differ only in the position of two strand amino acids (Fig. 1). Taking into account the turn sequence of these peptides, they may adopt two different types of β-hairpins, a 4:4 and a 3:5 (Fig. 2). The analysis of several NMR parameters, nonsequential NOEs, $^{13}C_\alpha$ conformational shifts, and $C_\alpha H$ conformational shifts, demonstrates that, in aqueous solution, peptide 3 adopts two folded structures, a 4:4 and a 3:5 β-hairpin, and peptide 4 only forms a 3:5 β-hairpin. The 3:5 β-hairpins formed by the peptides 3 and 4 are populated at a quite different extent (Table 1). A change in the position of two amino acids at the N-terminal strand greatly affects the conformational properties of the peptides. It has already been shown that the geometry of the type I + G1 β-bulge turn present in the 3:5 β-hairpin is more appropriate for β-hairpin formation than the topology of the type I β-turn present in 4:4 β-hairpins (de Alba et al., 1997b). Therefore, it is reasonable that, as experimentally found, peptides 3 and 4 having the same sequence in the turn region and the same amino acid composition in the strands are both able to adopt a 3:5 β-hairpin, whereas only peptide 3 forms a 4:4 β-hairpin. The fact that there was no correlation between an increase in the population of 4:4 β-hairpin and a decrease in the population of 3:5 β-hairpin in a series of 10-residue peptides (de Alba et al., 1997b) suggested that the formation of 4:4 and 3:5 β-hairpins is, to a first approach, independent of each other. Mak-

ing this assumption, it is feasible to analyze the factors affecting the formation of each hairpin independently.

Among the several factors that contribute to the overall stability of 4:4 β-hairpins, the intrinsic β-sheet, and β-turn propensities, the hydrogen-bonding network and cross-strand side chain–side chain interactions, though the location of two of them differs, are identical for peptides 3 and 4. In the case of 3:5 β-hairpins, the cross-strand side chain–side chain interactions are different for peptides 3 and 4. The packing of side chains on one face of the 4:4 β-hairpin, which were composed of residues 1, 3, 5, 10, 12, and 14, and on one face of the 3:5 β-hairpin, which was formed by residues 1, 3, 5, 11, 13, and 15, is different in peptides 3 and 4 (Fig. 2). This, in turn, could lead to differences in buried hydrophobic surface areas. Lower stability would be expected for the β-hairpin that buries less hydrophobic surface area upon formation. The burial of hydrophobic surface area has been proposed to contribute to the 2:2 β-hairpin stability in other model peptides (Ramírez-Alvarado et al., 1996; Maynard et al., 1998; Griffiths-Jones et al., 1999). To check if, in our peptide system, the hydrophobic effect is responsible for the stability differences observed between the two 4:4 β-hairpins and the two 3:5 β-hairpins, we have built four sets of model structures, corresponding to the ideal 4:4 and 3:5 β-hairpins for the sequences of peptides 3 and 4 (see Materials and methods). The hydrophobic surface areas buried for the two sets of 4:4 β-hairpins modelled as well as for the sets of 3:5 β-hairpins are very similar and within the experimental error. They are also very close to the hydrophobic surface area buried upon formation of the 3:5 β-hairpin structure adopted by peptide 4, as calculated on the basis of the NMR experimental restraints. Therefore, although these results do not constitute definitive evidence, they suggest that the hydrophobic effect does not account either for the distinctive abilities of peptides 3 and 4 to adopt a 4:4 β-hairpin or for the differences in 3:5 β-hairpin stability between peptides 3 and 4. If the hydrophobic effect contribution to the experimentally observed differences in β-hairpins stability is negligible, the remaining distinctive factors that can play a role in β-hairpin formation are the nature and location of cross-strand interactions.

As a consequence of our design strategy, the potential 4:4 β-hairpin for peptide 4 differs from that adopted by peptide 3 only in the position of S-T and I-T interactions relative to the turn (Table 1; Fig. 2). Both interactions are at hydrogen-bonded sites. When the favorable S-T interaction (de Alba et al., 1997b) is adjacent to the turn, as occurs in peptide 3, the 4:4 β-hairpin is present in aqueous solution. In contrast, no population of 4:4 β-hairpin is detected for peptide 4 where the favorable S-T interaction is shifted to the middle of the strands and the unfavorable I-T interaction (de Alba et al., 1997b) is adjacent to the turn. This result parallels the conformational behavior previously found for peptides 1 and 2 relative to 4:4 β-hairpin formation (Table 1; de Alba et al., 1997b). In these shorter peptides, the terminal location of the stabilizing S-T interaction in the 4:4 β-hairpin expected for peptide 2 suggests that fraying is the main reason that the interaction is inefficient at stabilizing the hairpin. However, the fraying effect is minimized in peptide 4 where the stabilizing S-T interaction is at the middle of the strands (Table 1). Thus, the differential ability of peptides 3 and 4 to adopt a 4:4 β-hairpin suggests that the effects of cross-strand side-chain interactions on β-hairpin formation do depend on their proximity to the turn. A destabilizing interaction, such as I-T, adjacent to the turn can hinder β-hairpin formation, if the turn topology is not very appropriate for β-hairpin formation as occurs in 4:4 β-hairpins, while the efficiency of a stabilizing interaction, such as S-T, can be larger when adjacent to the turn.

Analysis of cross-strand interactions in the adopted 3:5 β-hairpins is not straightforward, because the position swap between S and I leads to different interactions and not just to a change in their location relative to the turn. The 3:5 β-hairpin formed by peptide 3 contains the I-V and S-W interactions in a nonhydrogen-bonded site and peptide 4, S-V, and I-W (Table 1). Considering statistical analysis of pairwise interactions in antiparallel β-sheets (Wouters & Curmi, 1995; Hutchinson et al., 1998), I-V in a nonhydrogen-bonded site is favorable and S-V unfavorable. Data for S-W and I-W in a nonhydrogen-bonded site, which are not statistically significant, suggest an almost equal and null effect of these interactions on β-sheet stability. According to this, S-W and I-W, the interactions closer to the turn, will contribute equally to β-hairpin formation. Then, the population of 3:5 β-hairpin should be higher in peptide 3, which contains the favorable I-V interaction than in peptide 4 with the unfavorable S-V, but the opposite result is experimentally found (Table 1). A reasonable explanation comes from the fact that the I residue, which has higher intrinsic β-sheet propensity than S, is closer to the turn region in peptide 4 than peptide 3, suggesting that residues with higher intrinsic β-sheet propensities are more effective when closer to the turn. This is in analogy to the conclusions about the larger effectiveness of the cross-strand interactions when closer to the turn previously deduced from the 4:4 β-hairpins. It might also be possible that the interaction I-W is more stabilizing than S-W, and that this could not be inferred as a consequence of shortage of data in the statistical analysis. If so, the effect of cross-strand side-chain interactions on β-hairpin formation would depend on their proximity to the turn. The effectiveness of the interaction I-W in stabilizing the 3:5 β-hairpin formed by peptide 4 could be related to the fact that I and W are the two largest hydrophobic side chains. In any case, the stabilizing contributions from the closer residues to the turn appear to be more important in β-hairpin formation.

Considering the clear-cut results on 4:4 β-hairpins and those on 3:5 β-hairpins, we suggest that the contribution to β-hairpin formation of stabilizing and destabilizing factors, i.e., cross-strand side chain–side chain interactions and intrinsic β-sheet propensities, is likely more important when closer to the turn region. This is in agreement with the essential role of the turn sequence in nucleating β-hairpin folding as supported by experimental results (de Alba et al., 1997a, 1997b, 1999a, 1999b; Griffiths-Jones et al., 1999) and proposed by theoretical studies (Muñoz et al., 1997, 1998). If the turn sequence directs β-hairpin formation by predisposing the orientation of the two β-strands, it is reasonable that a stabilizing interaction between the two residues adjacent to the turn favors the formation of that β-hairpin. Our conclusion could also explain the different mutational tolerance displayed by two exposed residue pairs belonging to two β-hairpins of the β-barrel protein CspA (Zaremba & Gregoret, 1999), since, as we would expect, the less tolerant pair was that closer to the turn region. Nevertheless, the fact that this pair belongs to a nonhydrogen-bonded site and the other to a hydrogen-bonded site must also be considered, since it may contribute to the differential behavior of the two pairs, as suggested by Zaremba and Gregoret (1999). Our proposal also agrees with the amino acid β-sheet intrinsic propensities being context-dependent as indicated by the discrepancies found among different experimental determinations (Kim & Berg, 1993; Minor & Kim, 1994; Smith et al., 1994). Statistical analysis of pairwise interactions in antiparallel β-sheets have distinguished

between hydrogen- and nonhydrogen-bonded positions, with no consideration about the linker between the two antiparallel strands (Wouters & Curmi, 1995; Hutchinson et al., 1998). Moreover, the only reported survey of side-chain interactions in β-hairpins (Gunasekaran et al., 1997) does not take into account any positional effect. Statistical analysis of pairwise interactions in β-hairpins of known protein structures that consider the position dependence of cross-strand interactions, as suggested by our results, will be useful to test the general validity of our conclusion.

Conclusion

In brief, the conformational behavior of two designed 15-residue β-hairpin-forming linear peptides suggests that the contribution of stabilizing and destabilizing factors, such as cross-strand side-chain interactions, to β-hairpin formation depends on the relative position of the pair with respect to the turn. The strand residues adjacent to the turn appear to be the most relevant for β-hairpin formation, which is in agreement with previous results indicating the essential role of the turn region for β-hairpin formation. This positioning effect might be contributing to the context dependence found for amino acid intrinsic β-sheet propensities.

Materials and methods

Peptide synthesis and purification.

Peptides 3 and 4 were chemically synthesized by the Peptide Synthesis Facility at the Department of Organic Chemistry (University of Barcelona, Spain).

Sedimentation equilibrium

Sedimentation equilibrium experiments were performed to obtain the average molecular weight of peptide samples at ~0.2 mM concentration in aqueous solution at pH 5.5 and containing 150 mM NaCl to screen nonideal effects involving charged residues at high peptide concentrations. Peptide samples (70 μL) were centrifuged at 60,000 rpm at 278 K in 12 mm triple-sector Epon charcoal centrepieces, using a Beckman Optima XL-A ultracentrifuge with a Ti60 rotor. Radial scans were taken at different wavelengths every 2 h until equilibrium conditions were reached. The data were analyzed using the program XLAEQ from Beckman. The partial specific volumes of the peptides were calculated on the basis of their amino acid composition and corrected for temperature (Laue et al., 1992).

NMR spectra

Peptide samples for NMR experiments were prepared in 0.5 mL of H_2O/D_2O (9:1 ratio by volume) or in pure D_2O. Peptide concentrations were about 2 mM. pH was measured with a glass micro electrode and was not corrected for isotope effects. The temperature of the NMR probe was calibrated using a methanol sample. Sodium [3-trimethylsilyl 2,2,3,3-^{2}H] propionate (TSP) was used as an internal reference. The ^{1}H-NMR spectra were acquired on a Bruker AMX-600 pulse spectrometer operating at a proton frequency of 600.13 MHz. One-dimensional spectra were acquired using 32K data points, which were zero-filled to 64K data points before performing the Fourier transformation. Phase-sensitive 2D correlated spectroscopy (COSY) (Aue et al., 1976), total correlated spectroscopy (TOCSY) (Rance, 1987), NOE spectroscopy (NOESY) (Jeener et al., 1979; Kumar et al., 1980) and rotating frame NOE spectroscopy (ROESY) (Bothner-By et al., 1984; Braunschweiler & Ernst, 1983) spectra were recorded by standard techniques using presaturation of the water signal and the time-proportional phase incrementation mode (Redfield & Kuntz, 1975). NOESY and ROESY mixing times were 200 and 120 ms, respectively. TOCSY spectra were recorded using 80 ms MLEV17 with z filter spin-lock sequence (Rance, 1987). The ^{1}H-^{13}C heteronuclear single quantum coherence spectra (HSQC) (Bodenhausen & Ruben, 1980) at natural ^{13}C abundance were recorded in 2 mM peptide samples in D_2O. Acquisition data matrices were defined by 2,018 $\times$ 512 points in t_2 and t_1, respectively. Data were processed using the standard XWIN-NMR Bruker program on a Silicon Graphics computer. The 2D data matrix was multiplied by a square-sine-bell window function with the corresponding shift optimized for every spectrum and zero-filled to a 2 $\times$ 1K complex matrix prior to Fourier transformation. Baseline correction was applied in both dimensions. The 0 ppm ^{13}C δ was obtained indirectly by multiplying the spectrometer frequency that corresponds to 0 ppm in the ^{1}H spectrum, assigned to internal TSP reference, by 0.25144954 (Bax & Subramanian, 1986; Spera & Bax, 1991).

NMR assignment

The ^{1}H NMR signals of peptides 3 and 4 in aqueous solution were readily assigned by standard sequential assignment methods (Wüthrich et al., 1984; Wüthrich, 1986). Then, the ^{13}C resonances were straightforwardly assigned on the basis of the cross-correlations observed in the HSQC spectra between the proton and the carbon to which it is bonded. The ^{1}H and ^{13}C δ-values of the two peptides are available in Supplementary material in the Electronic Appendix (Tables SM1 and SM2) and have been deposited at the PESCADOR database (http://ucmb.ulb.ac.be/Pescador/).

Estimation of β-hairpin populations

The β-hairpin populations were estimated from the ratio of intensities of the $C_\alpha H_i$-$C_\alpha H_j$ NOE characteristic of each hairpin to that of the conformationally independent C_αH-$C_{\alpha'}$H Gly NOE, which was used with calibration purposes (Searle et al., 1995; de Alba et al., 1996, 1997a, 1997b; Ramírez-Alvarado et al., 1996; Maynard et al., 1998). The intensity ratio corresponding to a 100% β-hairpin was taken as $[d_{C\alpha H_i\text{-}C\alpha H_j}]^{-6}/[d_{C\alpha H\text{-}C\alpha' H\ Gly}]^{-6}$, where $d_{C\alpha H_i\text{-}C\alpha H_j}$ is the average $C_\alpha H_i$-$C_\alpha H_j$ distance in antiparallel β-sheets in proteins (2.3 Å; Wüthrich, 1986), where i and j are facing residues in a nonhydrogen-bonded site, and $d_{C\alpha H\text{-}C\alpha' H\ Gly}$ is the C_αH-$C_{\alpha'}$H distance characteristic of Gly residues (1.78 Å). NOE intensities were measured by volume integration in NOESY spectra (200 ms mixing time) recorded in pure D_2O samples.

The overall β-hairpin populations were independently evaluated by using the $\Delta\delta_{C\alpha H}$ ($\delta_{C\alpha H(\text{observed})} - \delta_{C\alpha H(\text{random coil})}$) and $\Delta\delta^{13}{}_{C_\alpha}$ ($\delta^{13}{}_{C_\alpha(\text{observed})} - \delta^{13}{}_{C_\alpha(\text{random coil})}$) conformational shifts averaged over all the strand residues in the adopted hairpins, except for the N- and C-terminal residues that would present charge end effects. The $\Delta\delta_{C\alpha H}$ conformational shift of residue 5 of peptides 3 and 4 was not included because the δ value of its C_αH proton is strongly affected for the aromatic ring of its facing W side chain in the 3:5 β-hairpin. The reference values for each residue in the random coil state were taken from Wüthrich (1986) for proton chemical shifts

($\delta_{C\alpha H(\text{random coil})}$) and from Wishart et al. (1995) for carbon chemical shifts ($\delta_{^{13}C_\alpha(\text{random coil})}$). The reference values for 100% β-hairpin were the mean conformational shifts reported for β-sheet proteins, 0.40 ppm for $\Delta\delta_{C\alpha H}$ (Wishart et al., 1991) and −1.48 ppm for $\Delta\delta_{^{13}C_\alpha}$ (Spera & Bax, 1991).

The ratio of the β-hairpin populations for each residue of peptide 4 was computed as the ratio $\Delta\delta_{C\alpha H(5°C)}/\Delta\delta_{C\alpha H(35°C)}$, where $\Delta\delta_{C\alpha H(5°C)}$ and $\Delta\delta_{C\alpha H(35°C)}$ are the $\Delta\delta_{C\alpha H}$ conformational shifts measured for each residue at 5 and at 35°C, respectively.

Structure calculation

Intensities of medium- and long-range NOEs were evaluated qualitatively and used to obtain upper limit distant constraints: strong (3.0 Å), intermediate between strong and medium (3.5 Å), medium (4.0 Å), intermediate between medium and weak (4.5 Å), weak (5.0 Å), and very weak (5.5 Å). Pseudo atom corrections were added where necessary. φ Angles were constrained to the range −180 to 0° except for Asn and Gly. For those residues with $^3J_{C\alpha H\text{-}NH} > 8.0$ Hz and $^3J_{C\alpha H\text{-}NH} < 5.0$ Hz, φ angles were restricted to the range −160 to −80°, and −100 to −20°, respectively. Structures were calculated on a Silicon Graphics computer using the program DIANA (Güntert et al., 1991).

Estimation of hydrophobic surface area buried upon β-hairpin formation

To model the 4:4 β-hairpins formed by peptide 3 and expected for peptide 4, a structure calculation was performed by using the DYANA program (Güntert et al., 1997) and introducing as distance and dihedral angle constraints those expected for an ideal 4:4 β-hairpin. For each sequence, the set of the 30 structures with the lowest target function was taken as model for the 4:4 β-hairpin. The same procedure was used to model the 3:5 β-hairpin adopted by peptides 3 and 4, but taking as distance and dihedral angle constraints those expected for an ideal 3:5 β-hairpin. The solvent-accessible nonpolar area for each structure was calculated using the program VADAR (Wishart et al., 1996). The hydrophobic surface area buried upon β-hairpin formation was computed as the difference between the solvent-accessible nonpolar area averaged over the 30 modeled structures and that corresponding to a completely extended structure. To obtain the hydrophobic surface area buried upon formation of the 3:5 β-hairpin formed by peptide 4, we followed the same procedure but using the 20 best structures calculated from experimental restraints (Fig. 5). The hydrophobic surface area buried upon formation of a 4:4 β-hairpin is 524 ± 66 Å^2 and 524 ± 62 Å^2 for peptides 3 and 4, respectively. That buried upon formation of the modeled 3:5 β-hairpins is 509 ± 40 Å^2 for peptide 3 and 499 ± 40 Å^2, for peptide 4, and upon formation of the 3:5 β-hairpin experimentally found for peptide 4, 545 ± 62 Å^2.

Supplementary material in the Electronic Appendix

Two tables listing the ^{1}H and ^{13}C δ values of peptides 3 and 4 (Tables SM1, SM2) and two tables listing the nonsequential NOEs observed for peptides 3 and 4 (Tables SM3, SM4).

Acknowledgments

We thank Mrs. C. López, Mr. A. Gómez, and Mr. L. de la Vega for technical assistance, and Drs. G. Rivas and C. Alfonso for their help with the sedimentation equilibrium experiments. We are also grateful to Dr. D.V. Laurents and Dr. F.J. Blanco for their critical reading of the manuscript. This work was supported by the Spanish DGICYT project no. PB98-0677 and European Project no. CEE B104-97-2086. C.M.S. is recipient of a predoctoral fellowship from Autonomous Community of Madrid, Spain.

References

Aue WP, Bertholdi E, Ernst RR. 1976. Two-dimensional spectroscopy. Application to NMR. *J Chem Phys 64*:2229–2246.

Aurora R, Rose GD. 1998. Helix capping. *Protein Sci 7*:21–38.

Baldwin RL. 1995. The α-helix formation by peptides of defined sequence. *Biophys Chem 55*:127–135.

Bax A, Subramanian J. 1986. Sensitivity-enhanced two-dimensional heteronuclear shift correlation NMR spectroscopy. *J Magn Reson 67*:565–570.

Blanco FJ, Jiménez MA, Herranz J, Rico M, Santoro J, Nieto JL. 1993. NMR evidence of a short linear peptide that folds into a β-hairpin in aqueous solution. *J Am Chem Soc 115*:5887–5888.

Blanco FJ, Ramírez-Alvarado M, Serrano L. 1998. Formation and stability of β-hairpin structures in polypeptides. *Curr Opin Struct Biol 8*:107–111.

Bodenhausen G, Ruben DJ. 1980. Natural abundance nitrogen-15 NMR by enhanced heteronuclear spectroscopy. *Chem Phys Lett 69*:185–189.

Bothner-By AA, Stephens RL, Lee JM, Warren CD, Jeanloz RW. 1984. Structure determination of a tetrasaccharide: Transient nuclear Overhauser effects in the rotating frame. *J Am Chem Soc 106*:811–813.

Braunschweiler L, Ernst RR. 1983. Coherence transfer by isotropic mixing: Application to proton correlation spectroscopy. *J Magn Reson 53*:521–528.

Buckley P, Edison AS, Kemple MD, Prendergast FG. 1993. The $^{13}C_\alpha$-NMR assignments of melittin in methanol, and chemical shift correlations with secondary structure. *J Biomol NMR 3*:639–652.

Bundi A, Wüthrich K. 1979. ^{1}H NMR parameters of the common amino acid residues measured in aqueous solution of linear tetrapeptides H-Gly-Gly-X-Ala-OH. *Biopolymers 18*:285–297.

Case DA, Dyson HJ, Wright PE. 1994. Use of chemical shifts and coupling constants in nuclear magnetic resonance structural studies on peptides and proteins. *Methods Enzymol 239*:392–416.

Chou PY, Fasman GD. 1974. Conformational parameters for amino acids in helical, β-sheet, and random coil regions calculated from proteins. *Biochemistry 13*:211–222.

de Alba E, Blanco FJ, Jiménez MA, Rico M, Nieto JL. 1995. Interactions responsible for the pH dependence of the β-hairpin conformational population formed by a designed linear peptide. *Eur J Biochem 233*:283–292.

de Alba E, Jiménez MA, Rico M. 1997a. Turn residue sequence determines β-hairpin conformation in designed peptides. *J Am Chem Soc 119*:175–183.

de Alba E, Jiménez MA, Rico M, Nieto JL. 1996. ^{1}H NMR conformational investigation of designed short linear peptides able to fold into β-hairpin structures in aqueous solution. *Fold Des 1*:133–144.

de Alba E, Rico M, Jiménez MA. 1997b. Cross-strand side-chain interactions versus turn conformation in β-hairpins. *Protein Sci 6*:2548–2560.

de Alba E, Rico M, Jiménez MA. 1999a. The turn sequence directs β-strand alignment in β-hairpins. *Protein Sci 8*:2234–2244.

de Alba E, Rico M, Jiménez MA. 1999b. De novo design of a monomeric three-stranded antiparallel β-sheet. *Protein Sci 8*:854–865.

de Dios AC, Pearson JG, Oldfield E. 1993. Secondary and tertiary structural effects on protein NMR chemical shifts: An ab initio approach. *Science 260*:1491–1496.

Gellman SH. 1998. Minimal model systems for β-sheet secondary structure in proteins. *Curr Opin Chem Biol 2*:717–725.

Griffiths-Jones SR, Maynard AJ, Searle MS. 1999. Dissecting the stability of a β-hairpin peptide that folds in water: NMR and molecular dynamics analysis of the β-turn and β-strand contributions to folding. *J Mol Biol 292*:1051–1069.

Gronenborn AM, Clore GM. 1994. Identification of N-terminal helix capping boxes by means of ^{13}C chemical shifts. *J Biomol NMR 4*:455–458.

Guerois R, Cordier-Oschsenbein F, Baleux F, Huynh-Dinh T, Neumann J-M, Sanson A. 1998. A conformational equilibrium in a protein fragment caused by two consecutive capping boxes: ^{1}H-, ^{13}C-NMR, and mutational analysis. *Protein Sci 7*:1506–1515.

Gunasekaran K, Ramakrishnan C, Balaram P. 1997. β-Hairpins in proteins revisited: Lessons for *de novo* design. *Protein Eng 10*:1131–1141.

Güntert P, Braun W, Wüthrich K. 1991. Efficient computation of three-dimensional protein structures in solution from nuclear magnetic resonance data using the program DIANA and the supporting programs CALIBA, HABAS, and GLOMSA. *J Mol Biol 217*:517–530.

Güntert P, Mumenthaler C, Wüthrich K. 1997. Torsion angle dynamics for NMR structure calculation with the new program DYANA. *J Mol Biol 273*:283–298.

Haque TS, Gellman SH. 1997. Insights into β-hairpin stability in aqueous solution from peptides with enforced type I′ and type II′ β-turns. *J Am Chem Soc 119*:2303–2304.

Hutchinson EG, Sessions RB, Thornton JM, Woolfson DN. 1998. Determinants of strand register in antiparallel β-sheets: The differences between backbone hydrogen-bonded and non-hydrogen-bonded residue pairs. *Protein Sci 7*:2287–2300.

Iwadate M, Asakura T, Williamson MP. 1999. C_α and C_β carbon-13 chemical shifts in proteins from an empirical database. *J Biomol NMR 13*:199–211.

Jeener J, Meier BH, Bachmann P, Ernst RA. 1979. Investigation of exchange processes by two-dimensional NMR spectroscopy. *J Chem Phys 71*:4546–4553.

Jiménez MA, Bruix M, González C, Blanco FJ, Nieto JL, Herranz J, Rico M. 1993. CD and ^{1}H-NMR studies on the conformational properties of peptide fragments from the C-terminal domain of thermolysin. *Eur J Biochem 211*:569–581.

Jiménez MA, Muñoz V, Rico M, Serrano L. 1994. Helix stop and start signals in peptides and proteins. The capping box does not necessarily prevent helix elongation. *J Mol Biol 242*:487–496.

Kim CA, Berg JM. 1993. Thermodynamic β-sheet propensities measured using a zinc-finger host peptide. *Nature 362*:267–270.

Koradi R, Billeter M, Wüthrich K. 1996. MOLMOL: A program for display and analysis of macromolecular structures. *J Mol Graphics 14*:51–55.

Kumar A, Ernst RR, Wüthrich K. 1980. A two-dimensional nuclear Overhauser enhancement (2D NOE) experiment for the elucidation of complete proton-proton cross-relaxation networks in biological macromolecules. *Biochem Biophys Res Commun 95*:1–6.

Lacroix E, Kortemme T, López de la Paz M, Serrano L. 1999. The design of linear peptides that fold as monomeric β-sheet structures. *Curr Opin Struct Biol 9*:487–493.

Laue TM, Shak BD, Ridgeway TM, Pelletier SL. 1992. Computer-aided interpretation of analytical sedimentation data for proteins. In: Harding SE, Rowe AJ, Horton JC, eds. *Analytical ultracentrifugation in biochemistry and polymer science*. Cambridge, UK: Royal Society of Chemistry. pp 90–125.

Lee MS, Cao B. 1996. Nuclear magnetic resonance chemical shift: Comparison of estimated secondary structures in peptides by nuclear magnetic resonance and circular dichroism. *Protein Eng 9*:15–25.

Lyu PC, Wemmer DE, Zhou HX, Pinker RJ, Kallenbach NR. 1993. Capping interactions in isolated α-helices: Position-dependent substitution effects and structure of a serine-capped peptide helix. *Biochemistry 32*:421–425.

Maynard AJ, Sharman GJ, Searle MS. 1998. Origin of β-hairpin stability in solution: Structural and thermodynamic analysis of the folding of a model peptide supports hydrophobic stabilization in water. *J Am Chem Soc 120*:1996–2007.

Merutka G, Dyson HJ, Wright PE. 1995. "Random coil" ^{1}H chemical shifts obtained as a function of temperature and trifluoroethanol concentration for the peptide series GGXGG. *J Biomol NMR 5*:14–24.

Minor DL Jr, Kim PS. 1994. Measurement of the β-sheet-forming propensities of amino acids. *Nature 367*:660–663.

Muñoz V, Henry ER, Hofrichter J, Eaton WA. 1998. A statistical mechanical model for β-hairpin kinetics. *Proc Natl Acad Sci USA 95*:5872–5879.

Muñoz V, Serrano L. 1994. Intrinsic secondary structure propensities of the amino acids, using statistical φ-ψ matrices: Comparison with experimental scales. *Proteins Struct Funct Genet 20*:301–311.

Muñoz V, Serrano L. 1997. Development of the multiple sequence approximation within the AGADIR model of α-helix formation: Comparison with Zimm-Bragg and Lifson-Roig formalisms. *Biopolymers 41*:495–509.

Muñoz V, Serrano L, Jiménez MA, Rico M. 1995. Structural analysis of peptides encompassing all α-helices of three α/β parallel proteins: Che-Y, Flavodoxin, and P21-Ras: Implications for a-helix stability and the folding of α/β parallel proteins. *J Mol Biol 247*:648–669.

Muñoz V, Thompson PA, Hofrichter JA, Eaton WA. 1997. Folding dynamics and mechanism of β-hairpin formation. *Nature 390*:196–199.

Ramírez-Alvarado M, Blanco FJ, Niemann H, Serrano L. 1997. Role of β-turn residues in β-hairpin formation and stability in designed peptides. *J Mol Biol 273*:898–912.

Ramírez-Alvarado M, Blanco FJ, Serrano L. 1996. *De novo* design and structural analysis of a model β-hairpin peptide system. *Nat Struct Biol 3*:604–612.

Ramírez-Alvarado M, Kortemme T, Blanco FJ, Serrano L. 1999. Beta-hairpin and beta-sheet formation in designed linear peptides. *Bioorg Med Chem 7*:107–111.

Rance M. 1987. Improved techniques for homonuclear rotating-frame and isotropic mixing experiments. *J Magn Reson 74*:557–564.

Redfield AG, Kuntz SD. 1975. Quadrature Fourier NMR detection: Simple multiplex for dual detection. *J Magn Reson 19*:250–254.

Scholtz JM, Baldwin RL. 1992. The mechanism of α-helix formation by peptides. *Annu Rev Biophys Biomol Struct 21*:95–118.

Searle MS, Williams DM, Packman LC. 1995. A short linear peptide derived from the N-terminal sequence of ubiquitin folds into a water-stable non-native β-hairpin. *Nat Struct Biol 2*:999–1006.

Sibanda BL, Blundell TL, Thornton JM. 1989. Conformation of β-hairpins in protein structures. A systematic classification with applications to modelling by homology, electron density fitting and protein engineering. *J Mol Biol 206*:759–777.

Sibanda BL, Thornton JM. 1985. β-Hairpin families in globular proteins. *Nature 316*:170–174.

Sibanda BL, Thornton JM. 1991. Conformation β-hairpins in protein structures. Classification and diversity in homologous structures. *Methods Enzymol 202*:59–82.

Smith CK, Regan L. 1997. Construction and design of β-sheets. *Acc Chem Res 30*:153–161.

Smith CK, Withka JM, Regan L. 1994. A thermodynamic scale for the β-sheet forming tendencies of amino acids. *Biochemistry 33*:5510–5517.

Spera S, Bax A. 1991. Empirical correlation between protein backbone conformation and C_α and C_β ^{13}C NMR chemical shifts. *J Am Chem Soc 113*:5490–5492.

Swindells MB, MacArthur MW, Thornton JM. 1995. Intrinsic φ, ψ propensities of amino acids, derived from the coil regions of known structures. *Nat Struct Biol 2*:596–603.

Syud FA, Espinosa JF, Gellman SH. 1999. NMR-based quantification of β-sheet populations in aqueous solution through use of reference peptides for the folded and unfolded states. *J Am Chem Soc 121*:11578–11579.

Szilágyi L. 1995. Chemical shifts in proteins come of age. *Prog Nucl Magn Reson Spectros 27*:325–443.

Wishart DS, Bigam CG, Holm A, Hodges RS, Sykes BD. 1995. ^{1}H, ^{13}C and ^{15}N random coil NMR chemical shifts of the common amino acids. I. Investigations of nearest neighbor effects. *J Biomol NMR 5*:67–81.

Wishart DS, Sykes BD. 1994. Chemical shifts as a tool for structure determination. *Methods Enzymol 239*:363–392.

Wishart DS, Sykes BD, Richards FM. 1991. Relationship between nnuclear magnetic resonance chemical shift and protein secondary structure. *J Mol Biol 222*:311–333.

Wishart DS, Willard L, Sykes BD. 1996. VADAR. Volume angles define s area, version 1.3. Edmonton: University of Alberta. Protein Engineering Network of Centres of Excellence.

Wouters MA, Curmi PM. 1995. An analysis of side chain interactions and pair correlations within antiparallel β-sheets: The differences between backbone hydrogen-bonded and non-hydrogen-bonded residue pairs. *Proteins 22*:119–131.

Wüthrich K. 1986. *NMR of proteins and nucleic acids*. New York: J. Wiley & Sons.

Wüthrich K, Billeter M, Braun W. 1984. Polypeptide secondary structure determination by nuclear magnetic resonance observation of short proton-proton distances. *J Mol Biol 180*:715–740.

Yao J, Dyson HJ, Wright PE. 1997. Chemical shift dispersion and secondary structure prediction in unfolded and partly folded proteins. *FEBS Lett 419*:285–289.

Zaremba SM, Gregoret LM. 1999. Context-dependence of amino acid residue pairing in antiparallel β-sheets. *J Mol Biol 291*:463–479.

Zhou NE, Kay CM, Sykes BD, Hodges RS. 1993. A single-stranded amphipathic alpha-helix in aqueous solution: Design, structural characterization, and its application for determining alpha-helical propensities of amino acids. *Biochemistry 32*:6190–6197.